

Word for Person: Zero-shot Composed Person Retrieval

Delong Liu¹, Haiwen Li¹, Zhicheng Zhao^{1,3,*}, Fei Su^{1,3}, Hongying Meng²
¹Beijing University of Posts and Telecommunications, ²Brunel University
³Beijing Key Laboratory of Network System and Network Culture

{liudelong, lihaiwen52, zhaozc, sufei}@bupt.edu.cn, hongying.meng@brunel.ac.uk

Abstract

Searching for specific person has great security value and social benefits, and it often involves a combination of visual and textual information. Conventional person retrieval methods, whether image-based or text-based, usually fall short in effectively harnessing both types of information, leading to the loss of accuracy. In this paper, a whole new task called Composed Person Retrieval (CPR) is proposed to jointly utilize both image and text information for target person retrieval. However, the supervised CPR must depend on very costly manual annotation dataset, while there are currently no available resources. To mitigate this issue, we firstly introduce the Zero-shot Composed Person Retrieval (ZS-CPR), which leverages existing domain-related data to resolve the CPR problem without reliance on expensive annotations. Secondly, to learn ZS-CPR model, we propose a two-stage learning framework, Word4Per, where a lightweight Textual Inversion Network (TINet) and a text-based person retrieval model based on fine-tuned Contrastive Language-Image Pre-training (CLIP) network are learned without utilizing any CPR data. Thirdly, a finely annotated Image-Text Composed Person Retrieval dataset (ITCPR) is built as the benchmark to assess the performance of the proposed Word4Per framework. Extensive experiments under both Rank-1 and mAP demonstrate the effectiveness of Word4Per for the ZS-CPR task, surpassing the comparative methods by over 10%. The code and ITCPR dataset will be publicly available at <https://github.com/Delong-liu-bupt/Word4Per>.

1. Introduction

Person retrieval [19, 49] aims to identify target person images from a large-scale person gallery. It comprises two popular directions: Image-based Person Retrieval (IPR) [31] and Text-based Person Retrieval (TPR) [24], which are dedicated to using images and texts commonly acquired in

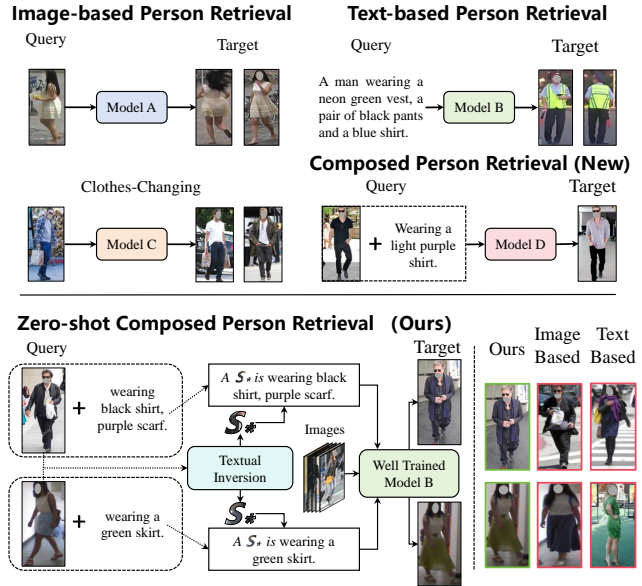


Figure 1. Existing methods and our proposed new task. **Top:** IPR aims to train a model (*Model A* and *Model C*) to identify the target person using a reference image, while TPR models (*Model B*) find the target person using text. Our proposed CPR task aims to use a supervised model (*Model D*) to identify the target by combining visual and textual information. **Bottom:** To avoid the use of costly triplets data for training *Model D*, we introduce the ZS-CPR task and present a solution.

daily life as queries to identify the targets of interest. In recent years, due to its extensive applications in video surveillance and public security, person retrieval has garnered increasing attention.

In real scenarios, when seeking a specific person, both visual and textual information are often available, while IPR and TPR methods can not fully leverage all information, inevitably leading to a certain loss in accuracy. Therefore, as shown in Figure 1, we propose a novel task, Composed Person Retrieval (CPR), to simultaneously utilize visual and textual information for retrieving the target person. The CPR task is a variant of the Composed Image Retrieval

*Corresponding author

(CIR) task [1], where the dataset consists of a large number of triplets (I_q, T_q, I_t) , comprising a reference image (I_q), a relative caption (T_q), and several target images (I_t). This type of data is manually collected and annotated and this process is time-consuming and expensive. Moreover, previous research [4, 16] in the CIR field has shown that training a fully supervised network (*Model D*) heavily depends on large-scale dataset, which is not available for the CPR task.

To address this challenge, we introduce a new task named as Zero-shot Composed Person Retrieval (ZS-CPR), aiming to present a new method that no longer relies on costly triplet annotations for supervised learning but rather uses existing image-caption data to solve the CPR issue. And correspondingly, a two-stage framework called Word4Per is proposed to learn the ZS-CPR model, image-caption datasets [8, 24, 55] for the TPR task are utilized. Specifically, in the first stage, cross-modal retrieval network [35] is applied to maximize the similarity between person images and their captions. In the second stage, a lightweight Textual Inversion Network (TINet) is constructed to map image into a special word. By this way, a flexible combination of reference image and relative caption for retrieval can be obtained. Furthermore, for effective evaluation the performance of Word4Per method, a test set ITCPR is constructed. The reference and target images in the ITCPR dataset reuse public person retrieval datasets such as CelebreID [17], LAST [38], and PRCC [47]. Annotating the relative captions is achieved by selecting images of the same identity with different outfits, and finally, a complete set of triplets is created.

As shown in Figure 1, in practical applications, the trained TINet is used to transform the reference image I_q into a pseudo-word S_* . Subsequently, this pseudo-word is concatenated via using a sentence template with the relative caption T_q . The well-trained *Model B* is then used for person retrieval, finding the corresponding targets.

To validate the effectiveness of our proposed the Word4Per framework and ITCPR dataset for the ZS-CPR task, extensive experiments are conducted. The experimental results show significant improvements in evaluation metrics compared to the state-of-the-art methods [19, 35]. The main contributions can be summarized as follows:

- A novel cross-modal task, named zero-shot composed person retrieval, is proposed to deal with the CPR problem without costly triplet annotations.
- We propose an efficient and flexible Word4Per framework for ZS-CPR, in which a lightweight textual inversion network and a TPR model are learned without utilizing any CPR triplets data.
- We annotate and build a new ITCPR dataset for the ZS-CPR task.
- Extensive experiments validate the effectiveness of our proposed Word4Per framework and ITCPR dataset.

2. Related work

2.1. Person Retrieval

Person retrieval consists of two main branches: IPR and TPR. IPR, the older subfield, has witnessed extensive research on feature extraction [31, 32, 39], metric learning [14], lightweight models [22, 34, 54], multi-branch methods [41, 49], and attention mechanisms [3, 50]. Recently, transformer-based models like PAT [27], DRL-Net [18], and TransReID [13] have gained popularity by combining ResNet-50 [12] with Transformer [40] decoders, achieving outstanding performance on large datasets. A recent popular variant of the IPR task is clothes-changing person retrieval [17], aimed at finding the same person with different clothing. This field has given rise to a plethora of datasets [17, 38, 47] and works [33, 46].

In contrast, TPR [24] is a relatively younger field, but it has progressed rapidly thanks to the development of text-image pre-training models [23, 35]. TPR aims to align image and text features in a shared embedding space to facilitate person matching. Early TPR methods [5, 53] primarily focused on extracting global [53] and local features [5, 48] from image-text pairs and then using matching loss for modality alignment. However they often struggled to balance efficiency and performance. Recent research [19, 28, 44] has introduced auxiliary tasks, to enable implicit feature alignment, thereby enhancing performance without increasing inference complexity. In [19], the pre-trained language-image model (CLIP) [35] was directly applied to TPR. However, the existing methods still do not effectively fused text and image information to find the target person, despite it is a common application.

2.2. Composed Image Retrieval

Composed Image Retrieval (CIR) [4, 16, 21] aims to achieve diverse image retrieval by merging image and text queries. This task belongs to the broader field of compositional learning [1, 6] and has been explored in various domains like fashion [11, 43] and scene composition [29], booming different fusion and training techniques. For instance, self-training shallow Transformers [40] and pre-trained Bert [7] models were utilized to fuse images and texts. However, these methods typically required training on carefully annotated CIR datasets [29, 43] and only performed effectively on images related to the training set. Consequently, the Zero-Shot Composed Image Retrieval (ZS-CIR) [2, 36] has been introduced. They leveraged the powerful modality alignment capabilities of big models like CLIP to convert image information into pseudo-text information [9], enabling the completion of the task without CIR dataset. Though the CPR task can be considered as a sub-task of CIR, the existing methods are not suitable for CPR.

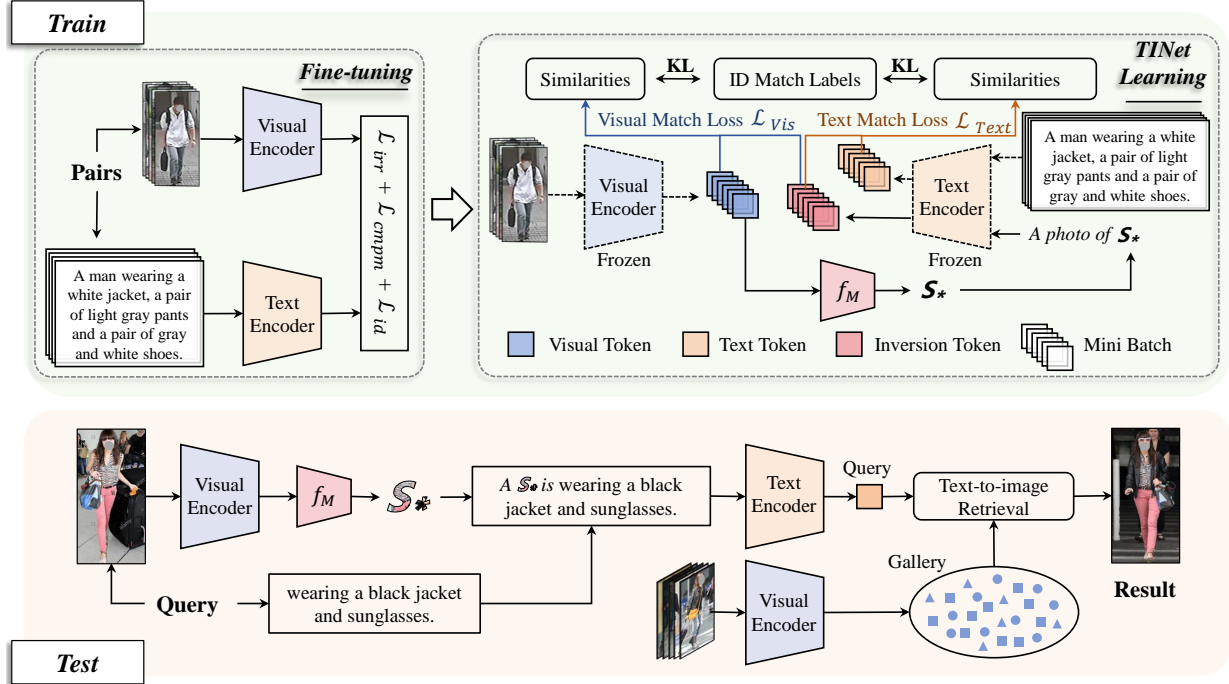


Figure 2. Training and inference of the Word4Per framework. **Top**: The training process is divided into two stages, and the first one is the fine-tuning phase, in which three losses (\mathcal{L}_{irr} [19], \mathcal{L}_{cmpm} [48], \mathcal{L}_{id} [53]) are used to optimize the visual and text encoders. The second stage is the training of the TINet f_M , where two contrastive learning losses \mathcal{L}_{Vis} and \mathcal{L}_{Text} are applied to supervise the generation of pseudo-word S_* . **Bottom**: During the testing phase, we use the well-trained dual encoders and TINet to accomplish CPR tasks.

3. Method

The proposed Word4Per framework is shown in Figure 2, and it consists of two main parts: fine-tuning the CLIP network and learning a TINet. Firstly, to align visual-textual features well, we fine-tune the CLIP network by introducing three supervised losses. Subsequently, a lightweight TINet is proposed to optimize the transformation of visual information into pseudo-word, where the visual and text encoders are frozen, and contrastive learning losses are employed. During the inference, the trained TINet is firstly used to generate pseudo-word token, which is then inserted into a sentence template along with the relative caption and fed into the text encoder, to produce the final text features for person retrieval.

3.1. Fine-tuning of CLIP Network

Considering that pre-training data of CLIP [35] is comprehensive and not specifically tailored for person retrieval, thus we fine-tune it based on image-caption data of person retrieval. In our implementation, we adopt an effective feature alignment network [19] to achieve this.

Fine-tuning of CLIP primarily solves identity issues of image-text pairs that are not covered in the pre-training, as well as finer details in person descriptions. To do this, different losses need to be introduced to supervise fea-

tures from different modalities, while aggregating different modality representations of the same identity, and emphasizing the fine-grained textual descriptions corresponding to images.

The whole fine-tuning of our Word4Per involves three supervised losses. Specifically, to discover finer relationships between image and text, an implicit relation reasoning loss \mathcal{L}_{irr} [19] is introduced. \mathcal{L}_{irr} is calculated by contrasting the probability distribution of words predicted using visual information with the actual distribution, and it is computed as follows:

$$\mathcal{L}_{irr} = -\frac{1}{|\mathcal{M}| \cdot |\mathcal{V}|} \sum_{i \in \mathcal{M}} \sum_{j \in |\mathcal{V}|} y_j^i \log \frac{\exp(m_j^i)}{\sum_{k=1}^{|\mathcal{V}|} \exp(m_k^i)}, \quad (1)$$

where \mathcal{M} represents a set of masked text tokens, $|\mathcal{V}|$ represents the vocabulary size, y_j^i is a one-hot vocabulary distribution where the ground-truth token has a probability of 1, and m_j^i is the predicted word distribution probability.

Moreover, aiming to match feature representations between different modalities, a cross-modal projection matching loss \mathcal{L}_{cmpm} [48] is adopted. \mathcal{L}_{cmpm} utilizes cosine similarity distributions to compute matching probabilities for $N \times N$ image-text pairs within a mini batch and employs KL divergence to measure the difference between these probabilities and the true matching labels. For each global em-

bedding f_i^v of an image, we can create a set of image-text embedding pairs $\{(f_i^v, f_j^t), l_{i,j}\}_{j=1}^N$, where $l_{i,j}$ is the true matching label. $l_{i,j} = 1$ indicates that (f_i^v, f_j^t) forms a matching pair from the same identity, while $l_{i,j} = 0$ denotes a non-matching pair. The cosine similarity between \mathbf{u} and \mathbf{v} , $\text{sim}(\mathbf{u}, \mathbf{v}) = \mathbf{u}^\top \mathbf{v} / \|\mathbf{u}\| \|\mathbf{v}\|$, is \mathcal{L}_2 normalized. The formula for calculating the matching probability is as follows:

$$p_{i,j} = \frac{\exp(\text{sim}(f_i^v, f_j^t) / \tau)}{\sum_{h=1}^N \exp(\text{sim}(f_i^v, f_h^t) / \tau)}, \quad (2)$$

where τ is a temperature hyperparameter controlling the peak of the probability distribution. Within a mini batch, the image-to-text matching loss is calculated using the following formula:

$$\mathcal{L}_{i2t} = KL(\mathbf{p}_i \| \mathbf{q}_i) = \frac{1}{N} \sum_{i=1}^N \sum_{j=1}^N p_{i,j} \log\left(\frac{p_{i,j}}{q_{i,j} + \epsilon}\right), \quad (3)$$

where ϵ is a small value to avoid numerical issues, and $q_{i,j} = l_{i,j} / \sum_{k=1}^N l_{i,k}$ represents the true matching probability.

Similarly, the text-to-image matching loss \mathcal{L}_{t2i} can be formalized by swapping f^v and f^t in equations (2) and (3), and the bidirectional matching loss \mathcal{L}_{cmpm} is calculated as follows:

$$\mathcal{L}_{cmpm} = \mathcal{L}_{i2t} + \mathcal{L}_{t2i}. \quad (4)$$

Furthermore, a common ID loss (\mathcal{L}_{id}) [53], is used to supervise identity label. Therefore, the overall optimization objective for the fine-tuning is:

$$\mathcal{L} = \mathcal{L}_{irr} + \mathcal{L}_{cmpm} + \mathcal{L}_{id}. \quad (5)$$

3.2. Learning the Textual Inversion Network

As mentioned before, the TINet is designed to achieve the mapping from image information to the linguistic space, where both image and word information in CLIP are represented by one-dimensional fixed-length vectors. Therefore, the TINet offers highly lightweight choice, allowing the mapping to be completed with minimal optimization complexity and optimal implementation speed. Specifically, in this paper, we opt for a shallow fully connected network. Based on image-text pairs, the TINet is learnt to map the global representation f_i^v of an image into pseudo-word token. Considering that the images and texts for the same identity are highly related, the loss function design for TINet optimization needs to include identity considerations.

As shown in the top of Figure 2, after completing the fine-tuning of the dual encoders, the training of the TINet is conducted with the dual encoders fully frozen. For the same batch of N image-text pairs, it is still able to construct a set of image-text representation pairs $\{(f_i^v, f_j^t), l_{i,j}\}_{j=1}^N$, where $l_{i,j}$ represents the real matching labels. The global

embedding f_i^v of each image is used to obtain pseudo-word embeddings as tokens $S_* = f_M(f_i^v)$. Subsequently, it is appended to the end of token embeddings of the prompt sentence, a photo of, resulting in \hat{S}_* . Then \hat{S}_* is fed into the text encoder to obtain textual inversion embedding $f_k^c, k = 1, 2, \dots, N$. Similarly, we obtain the set of embeddings for image and textual inversion pairs $\{(f_i^v, f_k^c), l_{i,k}\}_{k=1}^N$ and the corresponding set of text and textual inversion encoding pairs $\{(f_j^t, f_k^c), l_{j,k}\}_{k=1}^N$, where the real matching labels $l_{i,k}$ and $l_{j,k}$ are equal to the corresponding positions of $l_{i,j}$.

Through TINet, each pseudo-word embedding is expected to closely match the corresponding image. Therefore, the contrastive learning loss based on \mathcal{L}_{cmpm} is introduced to achieve this objective, i.e.,

$$\mathcal{L}_{Vis} = \mathcal{L}_{i2c} + \mathcal{L}_{c2i}, \quad (6)$$

$$\mathcal{L}_{Text} = \mathcal{L}_{t2c} + \mathcal{L}_{c2t}, \quad (7)$$

where \mathcal{L}_{i2c} is computed by replacing f^t with f^c in equations (2) and (3), \mathcal{L}_{c2i} is computed by replacing f^v with f^c and f^t with f^v , \mathcal{L}_{t2c} is computed by replacing f^v with f^t and f^t with f^c , and \mathcal{L}_{c2t} is computed by replacing f^v with f^c . The \mathcal{L}_{Vis} focuses more on visual information in the image, while the \mathcal{L}_{Text} focuses more on semantic information corresponding to the image.

Fine-tuning of CLIP and training of TINet are crucial for the Word4Per to acquire the combined zero-shot retrieval capability. TINet’s training relies on a highly aligned dual encoder, and the trained TINet can convert image information into pseudo-word that can be easily concatenated to sentences, thereby transforming the CPR task into a general TPR task implemented by fine-tuned CLIP. This is the key for Word4Per to accomplish ZS-CPR task.

3.3. Inference

During inference, a reference image with a relative caption is combined to find the target person among gallery images. As shown in the bottom of Figure 2, the query consists of two parts: an image and a textual caption. The image query passes through the visual encoder and the TINet f_M sequentially to obtain the inverted word S_* . Then, the query information is concatenated by using a sentence template a $[S_*]$ is {Caption}, and finally, the concatenated sentence serves as a text query to search for the target image in the gallery. Note that our approach is highly flexible during both training and testing phases, making it easy to strike a balance between performance and efficiency in real-world applications, and we discuss it in detail in the supplementary materials.

4. Datasets

In this section, a comprehensive overview for the ITCPR dataset is provided, and other related person retrieval

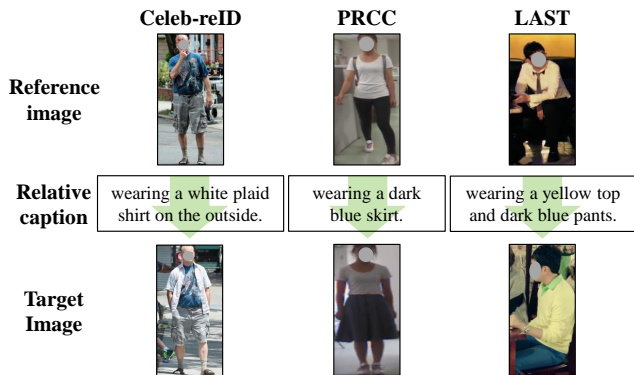


Figure 3. Examples of queries and ground truths in our ITCPR dataset.

datasets employed in experiments are also given.

4.1. ITCPR Dataset

In contrast to existing CIR datasets [29, 43], where reference and target images only need to be loosely related, the CPR datasets subject to the constraint that both of them depict the same person. Therefore, when constructing the ITCPR dataset, we require that the selected images to have the same identity, but wear different clothes or be in different scenes. Ultimately, publicly available clothes-changing datasets such as Celeb-reid [17], PRCC [47], and LAST [38] are utilized as our image sources.

The annotation process consists of several steps. The first step involves obtaining identities that have multiple images with different clothes to provide a diverse selection in subsequent steps. Next, two images are selected from the ones associated with each chosen identity and are denoted as I_q and I_t . Annotations that exclusively capture the distinctions between I_q and I_t , denoted as T_q , are manually crafted. Note that, the two images should ideally characterize partially matching costume, allowing I_q to provide additional clothing-related information beyond facial features and body posture. This additional clothing information will not be mentioned in annotation T_q , ensuring that CPR methods can only correctly identify I_t by making use of both I_q and T_q . After that, we obtain multiple triplets (I_q, T_q, I_t) for composed person retrieval. To prevent false negative cases, the gallery images are screened and re-annotated in the dataset (Supplementary B.1 for details). Some examples of ITCPR dataset are illustrated in Figure 3.

In summary, ITCPR comprises a total of 2,225 annotated triplets. These triplets encompass 2,202 unique combinations (I_q, T_q) as queries. ITCPR contains 1,151 images and 512 identities from Celeb-reID [17], 146 images and 146 identities from PRCC [47], and 905 images and 541 identities from LAST [38]. In the target gallery, there are a total of 20,510 images of persons from the three datasets,

with 2,225 corresponding ground truths for the queries. The mentioned annotations are exclusively designated for testing in the ZS-CPR task. Based on ITCPR dataset, the ZS-CPR task expects that methods can achieve substantial performance without utilizing any data from the three datasets mentioned above.

4.2. Other Datasets

Image-Caption Dataset. The Word4Per method employs image-caption datasets for both fine-tuning and TINET training. Notably, there are three publicly accessible datasets: CUHK-PEDES [24], ICFG-PEDES [8], and RST-PReid [55]. Our primary concern focuses on the CUHK-PEDES dataset, while the other two datasets are mainly employed for ablation experiments.

Image Datasets. In the Word4Per method, when exclusively utilizing \mathcal{L}_{Vis} for textual inversion optimization, the training uses the datasets containing only images. It’s essential to mention that datasets containing images of persons are abundant and widely available in IPR, including Market1501 [51], MSMT17 [42], CUHK02 [25], CUHK03-NP [26], CUHK-SYSU [45], GRID [30], VIPeR [10], QMUL i-LIDS [52], and PRID [15]. In subsequent ablation experiments, we combine above datasets with the images from image-caption datasets mentioned before to yield a total of 1,057,361 images, is collectively called the IPR dataset.

5. Experiments

5.1. Experiments Setup

Implementation Details. The experiments are conducted on a single A100 GPU. The input image size is adjusted to 384×128 , with each image patch measuring 16×16 . The maximum length for text tokens is set to 77. Training is performed by the Adam [20] optimizer for 60 epochs, with a batch size of 128. Cosine learning rate decay is applied. Initially, 5 warm-up epochs are conducted, gradually increasing the learning rate from 1/10 of the initial learning rate to the initial value. The temperature parameter τ in the losses is set to 0.02.

During the fine-tuning, the image and text encoders are initialized with pretrained CLIP [35] parameters. The initial learning rate is set to 10^{-5} . For modules with random initialization, the initial learning rate is set to 5×10^{-5} . In the training of the TINET, the parameters of the visual and text encoder inherit the fine-tuned parameters and remain frozen. A three-layer fully connected neural network is used to construct a lightweight TINET. When the visual encoder is ViT-B/16, the input and output dimensions are set to 512. When it is ViT-L/14, the input and output dimensions are 768, while the hidden layer dimension remains at 512. The parameters are randomly initialized. The initial learning rate is set to 10^{-4} . The CUHK-PEDES [24] dataset

No.	Backbone	Pretrain	Method	Rank-1	Rank-5	Rank-10	mAP	
1	ViT-B/16	CLIP [35]	Image-only	7.357	16.803	22.934	12.524	
2			Text-only	4.632	10.309	14.759	8.116	
3			Image+Text	16.757	32.516	40.372	24.674	
4		Fine-tuned		Image-only	5.041	10.763	13.442	8.086
5				Text-only	26.385	46.458	56.267	36.132
6				Image+Text	29.837	50.136	59.037	39.632
7				Ours (\mathcal{L}_{Vis})	<u>36.376</u>	<u>57.584</u>	<u>66.394</u>	<u>46.456</u>
8				Ours (\mathcal{L}_{Text})	40.054	61.262	68.574	49.903
9	ViT-L/14	CLIP [35]	Image-only	8.265	18.483	24.523	13.795	
10			Text-only	3.270	9.219	14.532	6.929	
11			Image+Text	18.165	35.195	43.324	26.652	
12			Pic2Word [36]	21.208	37.148	44.505	29.108	
13		Fine-tuned		Image-only	5.268	10.763	13.987	8.345
14				Text-only	28.974	50.817	59.900	39.333
15				Image+Text	32.016	52.634	60.990	41.831
16				Pic2Word [36] †	32.652	55.041	62.807	43.086
17				Ours (\mathcal{L}_{Vis})	<u>42.961</u>	<u>64.668</u>	<u>72.207</u>	<u>53.069</u>
18				Ours (\mathcal{L}_{Text})	45.549	66.803	74.796	55.260

Table 1. Zero-shot retrieval results of relevant methods on the ITCPR dataset. \mathcal{L}_{Vis} and \mathcal{L}_{Text} represent the losses used for supervised optimization of the TINet. The † symbol indicates that the training of the Pic2Word [36] method was performed on the original pre-trained parameters of CLIP [35], which may pose challenges for domain generalization and result in certain performance degradation.

is used for training, and if the visual encoder is ViT-B/16, the training takes approximately 5 hours, and if is ViT-L/14, the training takes about 11 hours. Because the dual encoder is frozen, storing the image-text features used for training in advance will save TINet’s training resources and speed several times.

Datasets. In this part, CUHK-PEDES is used as the default training dataset unless a special mention. In the subsequent ablation experiments, we abbreviate datasets as follows, CUHK-PEDES is denoted as C , ICFG-PEDES as I , and RSTPReid as R .

Evaluation Metrics. For ZS-CPR testing metrics, performance is evaluated by the Rank-k measure. This measure is employed to assess the probability of finding at least one matching person image among the top-k similar candidates for given query. Common values for k are 1, 5, and 10. Higher Rank-k scores indicate that the system effectively retrieves targets. In addition, we also employ the mean average precision (mAP) for evaluation. mAP is computed by calculating the average precision of retrieved relevant images and averaging the results across all queries, considering the performance of model on various queries. Higher Rank-k and mAP values signify superior method performance.

5.2. Quantitative Results

Word4Per is compared with several baseline methods [19, 35] that support zero-shot retrieval, as well as

Pic2Word [36], a method with notable performance in the ZS-CIR task. The baseline methods include several testing modes: 1) Image-only: using only the reference image via a pre-trained visual encoder to retrieve person. 2) Text-only: using only relative caption via a pre-trained text encoder. 3) Image + Text: Target person retrieval by averaging features obtained from the above two methods. 4) Pic2Word: using the parameters of the TINet trained with the original CIR method. Our method is trained and tested on both ViT-B/16 and ViT-L/14 visual encoders. Because Pic2Word is only provided for the ViT-L/14 scheme, thus we conduct the comparison with Pic2Word only under the ViT-L/14 experimental setting.

Table 1 shows the test results of comparative methods on the ITCPR dataset, demonstrating that our method significantly outperforms all baseline models and Pic2Word. The experimental results of No. 1-6, No. 9-11, and No. 13-15 reveal that utilizing both text and image information, regardless of whether the encoder is trained with CLIP [35] or fine-tuning, leads to optimal performance. This results also show the rational construction of our ITCPR dataset, leveraging both textual and visual cues from the query, the target person can be effectively identified. Comparing with the results of experiments No. 1-3 with No. 4-6, and No. 9-11 with No. 13-15, it is evident that fine-tuning the dual encoders is effective and necessary. Moreover, the results of No. 7-8 and No. 17-18 indicate that supervising the TINet with \mathcal{L}_{Text} is the most efficient, while this loss can only

No.	Method	Loss	Rank-1	Rank-5	Rank-10	mAP
1	\mathcal{L}_{Vis}	ITC	34.968	55.540	64.532	44.877
2		CMPM	36.376	57.584	66.394	46.456
3	\mathcal{L}_{Text}	ITC	36.648	60.082	68.256	47.455
4		CMPM	40.054	61.262	68.574	49.903

Table 2. Impact of different forms of loss functions

No.	Method	Dataset	Rank-1	Rank-5	Rank-10	mAP
1	Random	-	25.749	45.822	55.767	35.581
2	Text-only	-	26.385	46.458	56.267	36.132
3	\mathcal{L}_{Vis}	10%	31.608	53.270	61.399	41.722
4		20%	32.425	54.042	62.807	42.573
5		30%	33.106	54.541	62.988	43.151
6		50%	34.242	56.040	65.259	44.744
7		75%	36.785	58.220	66.757	46.934
8	100%	36.376	57.584	66.394	46.456	
9	\mathcal{L}_{Text}	10%	32.970	51.680	59.310	41.727
10		20%	34.242	55.040	63.259	43.744
11		30%	35.195	55.632	64.124	44.650
12		50%	37.125	57.026	65.468	46.951
13		75%	38.583	59.819	67.813	48.631
14		100%	40.054	61.262	68.574	49.903

Table 3. Impact of extracting data at different proportions from the same dataset for training. ‘‘Random’’ indicates the usage of randomly initialized TINet.

be employed for optimization when training with image-caption datasets, limiting the extensibility of the data.

5.3. Ablation Studies

To further show the effectiveness of the proposed Word4Per method for the ZS-CPR problem, we conduct extensive ablation studies. Due to limited training resources, the majority of ablation experiments are conducted on the fine-tuned dual encoders with a visual encoder of ViT-B/16. Note that experiments without specifying the dual encoders are based on this setup, and the parameters of the encoders are obtained from the fine-tuning network and remain frozen.

Effectiveness of the Loss Function. A comparison is made between the CMPM [19] loss and the Image-Text Contrastive (ITC) [36, 44] loss, which is commonly used in the CIR task. The results, as shown in Table 2, demonstrate that superior performance is consistently achieved by employing the CMPM loss with supervised optimization method. This also indicates that, for the CPR task, it is not appropriate to treat each image-text pair as an individual category but rather to consider all image-text pairs of the same identity as a single category, as they share all characteristics, including attire.

Word4Per with Smaller Data Volumes. We conduct

No.	Method	Dataset	Rank-1	Rank-5	Rank-10	mAP
1	\mathcal{L}_{Text}	C	40.054	61.262	68.574	49.903
2		I	34.242	57.084	65.077	44.803
3		R	33.878	55.631	63.352	43.996
4		$C + I$	35.559	56.676	64.033	45.371
5		$C + R$	34.877	55.904	63.397	44.760
6		$C + I + R$	38.193	59.310	67.302	48.120
7	\mathcal{L}_{Vis}	C	36.376	57.584	66.394	46.456
8		$C + I + R$	38.692	57.902	64.850	47.369
9		IPR	35.014	57.720	66.440	45.596
10		$IPR^{20\%+}$	38.227	59.192	66.893	48.219
11		$IPR^{10\%+}$	38.465	59.401	67.257	48.371
12		$IPR^{5\%+}$	38.147	58.265	65.985	47.600

Table 4. Impact of optimizing TINets with different datasets and methods. IPR represents the image dataset as described in Section 4.2, and $IPR^{20\%+}$ indicates selecting the largest 20% in terms of resolution to form a new dataset, with other cases following suit.

training of the TINet by extracting original data at different proportions to observe if utilizing more data will yield better results. As shown in Table 3, the experimental results show that even when using a randomly initialized TINet, it does not result in significant performance loss (No. 1 and No. 2). With a small amount of data available for training (No. 3 and No. 9), Word4Per performance still surpasses all previous methods. Furthermore, the results of experiments No. 9-14 lead to the following conclusions: when optimizing the TINet under \mathcal{L}_{Text} supervision on the same dataset, training with more image-text pairs can result in superior performance. However, for \mathcal{L}_{Vis} supervised optimization (No. 3-8), this trend is not evident. Therefore, what factors should be considered when choosing training data?

Quality Trumps Quantity in Data. To address the question, we conduct experiments on various data. As shown in Table 4, the experimental results reveal that the optimal performance is not achieved by training on the largest-scale data under two different supervisions. Comparing with the results No. 1-6, it is evident that combining dataset CUHK-PEDES [24] with other datasets [8, 55] does not lead to a performance improvement, which is different from Table 3. There are two reasons for this. Firstly, in Table 3, the increase in data size is limited in the same dataset. Secondly, concatenating other datasets not only increases the data size but also introduces different annotation styles, posing challenges for the learning of the TINet. The results of No. 6 indicate that when data size reaches a certain scale, the challenge can be mitigated to some extent. According to the results of No. 7-12, we can observe that large-scale data does not guarantee the best performance. In fact, the network trained with a dataset containing 1.05 million person images performs the worst. We also find that a large number of images in IPR datasets exist either blurry (low resolution)

Image	Top-10	Image	Top-10
	<p>sunglasses pimp newspaper mustache himself smen handsome man cool readers</p>		<p>boots cowgirl boot tight jeans bluec farmers jean blues woman</p>
	<p>drink drinking drinks sweater gril occup snack thirsty juice buying</p>		<p>dresses bluet sandals straps streets businesses dress enjoying cleavage front</p>
	<p>business suit purple ocity lilac gentleman classy front indigo fabulous</p>		<p>pumps heels dresses grey handbags gray leather silver skirts skirt</p>

Figure 4. Top-10 vocabulary words most similar to pseudo-words in some images

or obscured persons. Hence, we filter images to retrain the network, and the results of No. 9-12 exactly indicate that training the TINet with the filtered dataset results in higher performance. As for the person images in the image-caption datasets, since corresponding sentences need to be manually annotated, they are often clearer. Consequently, training the TINet with images from the three image-text datasets leads to the highest Rank-1 metric (No. 8). In short, through the above comparison, we find that data quality is more important than the data quantity for both \mathcal{L}_{Text} -based and \mathcal{L}_{Vis} -specific learning.

6. Discussion

Based on above results, it is evident that a well-trained TINet can effectively transform the image into a single pseudo-word token and can concisely and efficiently combine the relative caption to improve CPR performance. However, what semantic information is contained in these pseudo-words and whether these pseudo-words can be replaced with existing words from the vocabulary? To address these questions, within the entire vocabulary we attempt to find the words that are most similar to the pseudo-words, so as to infer the relevant semantic information hidden in the pseudo-words (Supplementary A.2 for details).

Several results from testing with randomly selected images are shown in Figure 4. It becomes apparent that words similar to the pseudo-words can effectively describe the original image, containing various details about the people. These details include gender information (e.g., *man*, *woman*, *girl*), clothing details (e.g., *boots*, *sweater*, *dresses*), color descriptions (e.g., *blue*, *purple*, *indigo*), and items carried by the people (e.g., *newspaper*, *sunglasses*, *handbags*). Furthermore, the obtained words contain additional aspects, such as the state of the persons, style, spatial location, attire materials, etc. It is worth noting that, some vocabu-

No.	Backbone	Method	Rank-1	Rank-5	Rank-10	mAP
1	ViT-B/16	Text-only	26.385	46.458	56.267	36.132
2		1st Sim	27.884	49.001	57.856	37.955
3		\mathcal{L}_{Text}	40.054	61.262	68.574	49.903
4	ViT-L/14	Text-only	28.974	50.817	59.900	39.333
5		1st Sim	32.016	53.769	62.761	42.242
6		\mathcal{L}_{Text}	45.549	66.803	74.796	55.260

Table 5. Experimental results of replacing pseudo-word tokens with existing words. “1st Sim” indicates using words with the highest similarity to replace pseudo-word tokens for target retrieval.

lary may not directly describe the image, but certain parts of these words (bolded in the Figure 4) can be prompted to the corresponding image. This phenomenon may be owned to the usage of Byte Pair Encoding (BPE) [37] in the text encoding. By extending observation to top-50 even top-100 words, we can unearth more meaningful semantic information. This suggests that pseudo-word tokens obtained by the TINet are actually a combination of multiple meaningful semantic information and contain a variety of information.

If pseudo-word tokens are replaced with the most similar words from the vocabulary, will the results still be stable? To investigate this, relevant experiments are conducted, and the results are shown in Table 5. The results show although adding a valid word can bring some performance improvement, it is far less obvious than the use of pseudo-word tokens. The results are also quite comprehensible, that is, it is challenging to summarize a person image just using one existing word, whereas one pseudo-word token can accomplish this.

7. Outlook

In this paper, we address limitations in handling queries that involve both image and text information for person retrieval, through the introduction of CPR task. To overcome data annotation challenges in CPR, we put forward the ZS-CPR problem, eliminating reliance on expensive triplet annotations. Furthermore, a two-stage framework called Word4Per is developed to train ZS-CPR model, achieving very promising performance on our proposed TICPR dataset without the need for CPR datasets. Comprehensive ablation studies are also conducted on Word4Per, and a slice of valuable insights are obtained.

However, The proposed CPR task is still in its infancy, and there are many directions that can be optimized. For instance, our method does not explicitly focus on maintaining consistent facial and body features for the same person. In addition, based on this information to narrow the retrieval scope without sacrificing retrieval efficiency is also a valuable issue.

References

- [1] Aishwarya Agrawal, Jiasen Lu, Stanislaw Antol, Margaret Mitchell, C. Lawrence Zitnick, Dhruv Batra, and Devi Parikh. Vqa: Visual question answering. *arXiv: Computation and Language, arXiv: Computation and Language*, 2015. 2
- [2] Alberto Baldrati, Lorenzo Agnolucci, Marco Bertini, and Alberto Del Bimbo. Zero-shot composed image retrieval with textual inversion. *arXiv preprint arXiv:2303.15247*, 2023. 2
- [3] Tianlong Chen, Shaojin Ding, Jingyi Xie, Ye Yuan, Wuyang Chen, Yang Yang, Zhou Ren, and Zhangyang Wang. Abdnnet: Attentive but diverse person re-identification. In *2019 IEEE/CVF International Conference on Computer Vision (ICCV)*, 2019. 2
- [4] Yanbei Chen, Shaogang Gong, and Loris Bazzani. Image search with text feedback by visiolinguistic attention learning. In *2020 IEEE/CVF Conference on Computer Vision and Pattern Recognition (CVPR)*, 2020. 2
- [5] Yuhao Chen, Guoqing Zhang, Yujiang Lu, Zhenxing Wang, and Yuhui Zheng. Tipcb: A simple but effective part-based convolutional baseline for text-based person search. *Neurocomputing*, 494:171–181, 2022. 2
- [6] Marcella Cornia, Matteo Stefanini, Lorenzo Baraldi, and Rita Cucchiara. Meshed-memory transformer for image captioning. In *2020 IEEE/CVF Conference on Computer Vision and Pattern Recognition (CVPR)*, 2020. 2
- [7] Jacob Devlin, Ming-Wei Chang, Kenton Lee, and Kristina Toutanova. Bert: Pre-training of deep bidirectional transformers for language understanding. *arXiv preprint arXiv:1810.04805*, 2018. 2
- [8] Zefeng Ding, Changxing Ding, Zhiyin Shao, and Dacheng Tao. Semantically self-aligned network for text-to-image part-aware person re-identification. *arXiv preprint arXiv:2107.12666*, 2021. 2, 5, 7
- [9] Rinon Gal, Yuval Alaluf, Yuval Atzmon, Or Patashnik, Amit Haim Bermano, Gal Chechik, and Daniel Cohen-or. An image is worth one word: Personalizing text-to-image generation using textual inversion. In *The Eleventh International Conference on Learning Representations*, 2022. 2
- [10] Douglas Gray and Hai Tao. Viewpoint invariant pedestrian recognition with an ensemble of localized features. In *Computer Vision—ECCV 2008: 10th European Conference on Computer Vision, Marseille, France, October 12–18, 2008, Proceedings, Part I 10*, pages 262–275. Springer, 2008. 5
- [11] Xiaoxiao Guo, Hui Wu, Yu Cheng, Steven J. Rennie, Gerald Tesaro, and Rogerio Feris. Dialog-based interactive image retrieval. *arXiv: Computer Vision and Pattern Recognition, arXiv: Computer Vision and Pattern Recognition*, 2018. 2
- [12] Kaiming He, Xiangyu Zhang, Shaoqing Ren, and Jian Sun. Deep residual learning for image recognition. In *Proceedings of the IEEE conference on computer vision and pattern recognition*, pages 770–778, 2016. 2
- [13] Shuting He, Hao Luo, Pichao Wang, Fan Wang, Hao Li, and Wei Jiang. Transreid: Transformer-based object re-identification. In *2021 IEEE/CVF International Conference on Computer Vision (ICCV)*, 2021. 2
- [14] Alexander Hermans, Lucas Beyer, and Bastian Leibe. In defense of the triplet loss for person re-identification. *arXiv: Computer Vision and Pattern Recognition, arXiv: Computer Vision and Pattern Recognition*, 2017. 2
- [15] Martin Hirzer, Csaba Beleznai, Peter M Roth, and Horst Bischof. Person re-identification by descriptive and discriminative classification. In *Image Analysis: 17th Scandinavian Conference, SCIA 2011, Ystad, Sweden, May 2011. Proceedings 17*, pages 91–102. Springer, 2011. 5
- [16] Mehrdad Hosseinzadeh and Yang Wang. Composed query image retrieval using locally bounded features. In *2020 IEEE/CVF Conference on Computer Vision and Pattern Recognition (CVPR)*, 2020. 2
- [17] Yan Huang, Qiang Wu, Jingsong Xu, and Yi Zhong. Celebrities-reid: A benchmark for clothes variation in long-term person re-identification. In *2019 International Joint Conference on Neural Networks (IJCNN)*, pages 1–8. IEEE, 2019. 2, 5
- [18] Mengxi Jia, Xinhua Cheng, Shijian Lu, and Jian Zhang. Learning disentangled representation implicitly via transformer for occluded person re-identification. *IEEE Transactions on Multimedia*, 25:1294–1305, 2022. 2
- [19] Ding Jiang and Mang Ye. Cross-modal implicit relation reasoning and aligning for text-to-image person retrieval. In *Proceedings of the IEEE/CVF Conference on Computer Vision and Pattern Recognition*, pages 2787–2797, 2023. 1, 2, 3, 6, 7
- [20] Diederik P. Kingma and Jimmy Ba. Adam: A method for stochastic optimization. *arXiv: Learning, arXiv: Learning*, 2014. 5
- [21] Seungmin Lee, Dongwan Kim, and Bohyung Han. Cosmo: Content-style modulation for image retrieval with text feedback. In *2021 IEEE/CVF Conference on Computer Vision and Pattern Recognition (CVPR)*, 2021. 2
- [22] Hanjun Li, Gaojie Wu, and Wei-Shi Zheng. Combined depth space based architecture search for person re-identification. In *2021 IEEE/CVF Conference on Computer Vision and Pattern Recognition (CVPR)*, 2021. 2
- [23] Junnan Li, Dongxu Li, Caiming Xiong, and Steven Hoi. Blip: Bootstrapping language-image pre-training for unified vision-language understanding and generation. In *International Conference on Machine Learning*, pages 12888–12900. PMLR, 2022. 2
- [24] Shuang Li, Tong Xiao, Hongsheng Li, Bolei Zhou, Dayu Yue, and Xiaogang Wang. Person search with natural language description. In *Proceedings of the IEEE conference on computer vision and pattern recognition*, pages 1970–1979, 2017. 1, 2, 5, 7
- [25] Wei Li and Xiaogang Wang. Locally aligned feature transforms across views. In *Proceedings of the IEEE conference on computer vision and pattern recognition*, pages 3594–3601, 2013. 5
- [26] Wei Li, Rui Zhao, Tong Xiao, and Xiaogang Wang. Deepreid: Deep filter pairing neural network for person re-identification. In *Proceedings of the IEEE conference on computer vision and pattern recognition*, pages 152–159, 2014. 5

- [27] Yulin Li, Jianfeng He, Tianzhu Zhang, Xiang Liu, Yongdong Zhang, and Feng Wu. Diverse part discovery: Occluded person re-identification with part-aware transformer. In *Proceedings of the IEEE/CVF Conference on Computer Vision and Pattern Recognition*, pages 2898–2907, 2021. 2
- [28] Delong Liu and Haiwen Li. Unleashing the imagination of text: A novel framework for text-to-image person retrieval via exploring the power of words. *arXiv preprint arXiv:2307.09059*, 2023. 2
- [29] Zheyuan Liu, Cristian Rodriguez-Opazo, Damien Teney, and Stephen Gould. Image retrieval on real-life images with pre-trained vision-and-language models. In *2021 IEEE/CVF International Conference on Computer Vision (ICCV)*, 2021. 2, 5
- [30] Chen Change Loy, Tao Xiang, and Shaogang Gong. Multi-camera activity correlation analysis. In *2009 IEEE Conference on Computer Vision and Pattern Recognition*, pages 1988–1995. IEEE, 2009. 5
- [31] Hao Luo, Youzhi Gu, Xingyu Liao, Shenqi Lai, and Wei Jiang. Bag of tricks and a strong baseline for deep person re-identification. In *Proceedings of the IEEE/CVF conference on computer vision and pattern recognition workshops*, pages 0–0, 2019. 1, 2
- [32] Jingjing Qian, Wei Jiang, Hao Luo, and Hongyan Yu. Stripe-based and attribute-aware network: a two-branch deep model for vehicle re-identification. *Measurement Science and Technology*, page 095401, 2020. 2
- [33] Xuelin Qian, Wenxuan Wang, Li Zhang, Fangrui Zhu, Yanwei Fu, Tao Xiang, Yu-Gang Jiang, and Xiangyang Xue. Long-term cloth-changing person re-identification. In *Proceedings of the Asian Conference on Computer Vision*, 2020. 2
- [34] Ruijie Quan, Xuanyi Dong, Yu Wu, Linchao Zhu, and Yi Yang. Auto-reid: Searching for a part-aware convnet for person re-identification. In *2019 IEEE/CVF International Conference on Computer Vision (ICCV)*, 2019. 2
- [35] Alec Radford, Jong Wook Kim, Chris Hallacy, Aditya Ramesh, Gabriel Goh, Sandhini Agarwal, Girish Sastry, Amanda Askell, Pamela Mishkin, Jack Clark, et al. Learning transferable visual models from natural language supervision. In *International conference on machine learning*, pages 8748–8763. PMLR, 2021. 2, 3, 5, 6
- [36] Kuniaki Saito, Kihyuk Sohn, Xiang Zhang, Chun-Liang Li, Chen-Yu Lee, Kate Saenko, and Tomas Pfister. Pic2word: Mapping pictures to words for zero-shot composed image retrieval. In *Proceedings of the IEEE/CVF Conference on Computer Vision and Pattern Recognition*, pages 19305–19314, 2023. 2, 6, 7
- [37] Rico Sennrich, Barry Haddow, and Alexandra Birch. Neural machine translation of rare words with subword units. *arXiv preprint arXiv:1508.07909*, 2015. 8
- [38] Xiujun Shu, Xiao Wang, Xianghao Zang, Shiliang Zhang, Yuanqi Chen, Ge Li, and Qi Tian. Large-scale spatio-temporal person re-identification: Algorithms and benchmark. *IEEE Transactions on Circuits and Systems for Video Technology*, 32(7):4390–4403, 2021. 2, 5
- [39] Yifan Sun, Liang Zheng, Yi Yang, Qi Tian, and Shengjin Wang. *Beyond Part Models: Person Retrieval with Refined Part Pooling (and a Strong Convolutional Baseline)*, page 501–518. 2018. 2
- [40] Ashish Vaswani, Noam Shazeer, Niki Parmar, Jakob Uszkoreit, Llion Jones, AidanN. Gomez, Lukasz Kaiser, and Illia Polosukhin. Attention is all you need. *Neural Information Processing Systems, Neural Information Processing Systems*, 2017. 2
- [41] Pingyu Wang, Zhicheng Zhao, Fei Su, and Honying Meng. Ltireid: Factorizable feature generation with independent components for long-tailed person re-identification. *IEEE Transactions on Multimedia*, 2022. 2
- [42] Longhui Wei, Shiliang Zhang, Wen Gao, and Qi Tian. Person transfer gan to bridge domain gap for person re-identification. In *Proceedings of the IEEE conference on computer vision and pattern recognition*, pages 79–88, 2018. 5
- [43] Hui Wu, Yupeng Gao, Xiaoxiao Guo, Ziad Al-Halah, Steven Rennie, Kristen Grauman, and Rogerio Feris. Fashion iq: A new dataset towards retrieving images by natural language feedback. In *2021 IEEE/CVF Conference on Computer Vision and Pattern Recognition (CVPR)*, 2021. 2, 5
- [44] Yushuang Wu, Zizheng Yan, Xiaoguang Han, Guanbin Li, Changqing Zou, and Shuguang Cui. Lapscore: language-guided person search via color reasoning. In *Proceedings of the IEEE/CVF International Conference on Computer Vision*, pages 1624–1633, 2021. 2, 7
- [45] Tong Xiao, Shuang Li, Bochao Wang, Liang Lin, and Xiaogang Wang. End-to-end deep learning for person search. *arXiv preprint arXiv:1604.01850*, 2(2):4, 2016. 5
- [46] Peng Xu and Xiatian Zhu. Deepchange: A long-term person re-identification benchmark with clothes change. In *Proceedings of the IEEE/CVF International Conference on Computer Vision*, pages 11196–11205, 2023. 2
- [47] Qize Yang, Ancong Wu, and Wei-Shi Zheng. Person re-identification by contour sketch under moderate clothing change. *IEEE transactions on pattern analysis and machine intelligence*, 43(6):2029–2046, 2019. 2, 5
- [48] Ying Zhang and Huchuan Lu. Deep cross-modal projection learning for image-text matching. In *Proceedings of the European conference on computer vision (ECCV)*, pages 686–701, 2018. 2, 3
- [49] Yan Zhang, Binyu He, Li Sun, and Qingli Li. Progressive multi-stage feature mix for person re-identification. In *ICASSP 2021 - 2021 IEEE International Conference on Acoustics, Speech and Signal Processing (ICASSP)*, 2021. 1, 2
- [50] Zhizheng Zhang, Cuiling Lan, Wenjun Zeng, Xin Jin, and Zhibo Chen. Relation-aware global attention for person re-identification. *arXiv: Computer Vision and Pattern Recognition, arXiv: Computer Vision and Pattern Recognition*, 2019. 2
- [51] Liang Zheng, Liyue Shen, Lu Tian, Shengjin Wang, Jingdong Wang, and Qi Tian. Scalable person re-identification: A benchmark. In *Proceedings of the IEEE international conference on computer vision*, pages 1116–1124, 2015. 5
- [52] WS Zheng. S, gong, and t. Xiang, “Associating groups of people,” *BMVC*, 2009. 5

- [53] Zhedong Zheng, Liang Zheng, Michael Garrett, Yi Yang, Mingliang Xu, and Yi-Dong Shen. Dual-path convolutional image-text embeddings with instance loss. *ACM Transactions on Multimedia Computing, Communications, and Applications (TOMM)*, 16(2):1–23, 2020. [2](#), [3](#), [4](#)
- [54] Kaiyang Zhou, Yongxin Yang, Andrea Cavallaro, and Tao Xiang. Omni-scale feature learning for person re-identification. In *2019 IEEE/CVF International Conference on Computer Vision (ICCV)*, 2019. [2](#)
- [55] Aichun Zhu, Zijie Wang, Yifeng Li, Xili Wan, Jing Jin, Tian Wang, Fangqiang Hu, and Gang Hua. Dssl: Deep surroundings-person separation learning for text-based person retrieval. In *Proceedings of the 29th ACM International Conference on Multimedia*, pages 209–217, 2021. [2](#), [5](#), [7](#)

Word for Person: Zero-shot Composed Person Retrieval

Supplementary Material

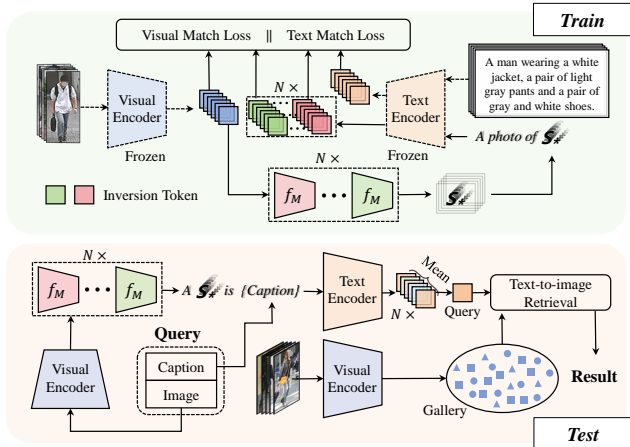


Figure A. Flexibility in Training and Inference. **Top:** The flexibility of the TINet training process allows the simultaneous and independent training of any number of f_M networks with different structures and loss supervision optimizations, using the same dataset. **Bottom:** The flexibility during the inference stage allows the combination of any number of TINet, regardless of their optimization process.

A. Method

A.1. Flexibility in Training and Testing.

Word4Per exhibits the flexibility both in training and testing phases. As shown in Figure A, during the training of the TINet, under the condition that the input data keeps consistent, multiple TINets f_M can be learnt simultaneously. Each f_M can be configured flexibly in terms of its structure and associated loss functions. Since the parameters of the visual encoder and text encoder remain frozen, each f_M will be updated solely based on respective loss function. This mode allows to share the frozen dual encoders in a single training process, reducing the number of times that the images and texts in the dataset pass through the encoders independently, enhancing efficiency.

During testing, our method becomes even more flexible. For example, it allows different number of networks with various structures, loss optimizations, and training data. After an image passes through the visual encoder, it can be processed by multiple TINets f_M to obtain multiple pseudo-words S_* , resulting in multiple final queries, whose average can yield the final query embedding and the corresponding retrieval result. In general, using more TINets can lead to better performance but lower efficiency. Therefore, different application requirements can find the balance between accuracy and efficiency.

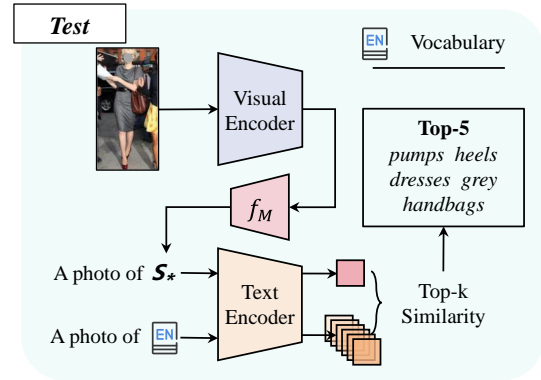


Figure B. Semantic information exploration of pseudo-word tokens. Experiments are conducted using the \mathcal{L}_{Text} supervised optimized TINets.

Furthermore, during the training of f_M , both \mathcal{L}_{Vis} and \mathcal{L}_{Text} are effective in learning the image information which includes visual and semantic types. The visual information is more specific, while the semantic information is more abstract, thus the optimization strategies for the two losses are should be different. Therefore, simply combining two losses for optimization does not guarantee the superior results (Table B). On the other hand, during joint testing with two different TINets optimized with distinct supervision, it is possible to freely select the network with better performance, making the performance improvement brought about by the fusion more stable.

A.2. Exploring Pseudo-Word Token Information.

Figure B shows the method used in Section 6 to find words most similar to pseudo-words. A well-trained visual encoder of ViT-B/16 is used for all shown cases (Figure 4).

B. Additional Details

B.1. ITCPR Datasets Re-annotation

A large number of noise images in gallery can potentially introduce false negative images. For example, for certain queries, some images could be potential ground truth but remain unlabeled. Incorporating such cases will decrease the reliability of the evaluation metrics. Therefore, as shown in Figure C, after completing the dataset annotation and adding noise images to the image gallery, we employ a well-trained visual encoder to search for the most similar images for each target image, followed by manual verification. By this way, we add corresponding annotations to

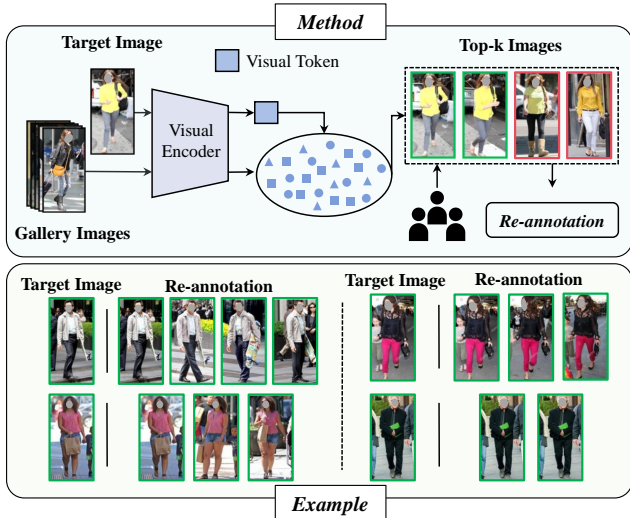


Figure C. False negative elimination scheme in ITCPR. **Top:** The method of eliminating false negative images and adding annotations in the dataset. **Bottom:** Examples of false negative images re-annotated in ITCPR.

eliminate false negatives, and the ITCPR dataset has been refined.

B.2. Image-Caption Dataset Details

CUHK-PEDES [24] comprises a total of 40,206 images and 80,412 textual descriptions from 13,003 identities. The training set includes 34,504 images, 11,003 identities, and 68,126 textual descriptions. The validation set consists of 3,078 images, 1,000 identities, and 6,158 textual descriptions. The test set includes 3,074 images, 1,000 identities, and 6,156 textual descriptions.

ICFG-PEDES [8] includes 54,522 textual descriptions corresponding to 54,522 images of 4,102 identities. Each image is associated with a single textual description, and the vocabulary consists of 5,554 unique words. The dataset is split into training and test sets with 34,674 image-text pairs of 3,102 identities, and 19,848 image-text pairs of the remaining 1,000 identities, respectively.

RSTPReid [55] contains 20,505 images from 4,101 different identities, captured by 15 cameras. Each identity has 5 images taken from different cameras, and each image is accompanied by a textual description containing no fewer than 23 words. For dataset partitioning, the training, validation, and test sets are composed of 3,701, 200, and 200 identities, respectively.

C. Additional Results

C.1. Fine-tuning Results

In the fine-tuning process of Word4Per, the objective is to make the model capable of performing TPR task effec-

No.	Backbone	Method	Rank-1	Rank-5	Rank-10	mAP
1	ViT-B/16	CLIP	12.606	27.112	35.559	11.145
2		Fine-tuned	73.847	89.571	93.681	68.086
3	ViT-L/14	CLIP	10.185	23.262	30.962	9.192
4		Fine-tuned	75.991	90.578	94.428	68.337

Table A. Performance of various pre-trained models on CUHK-PEDES [24]. Fine-Tune denotes the CLIP model fine-tuned according to the settings in this paper.

tively. In line with this, we also evaluate the performance of the fine-tuned models on the CUHK-PEDES test set, and the results are shown in Table A. It can be observed that fine-tuning the parameters of CLIP [35] is essential.

C.2. Qualitative Results

The visualization of the results obtained by ZS-CPR models are compared. Figure D shows two typical cases. In Case 1, it is evident that, regardless of the parameters scale, using image-only retrieval yields the poorest results. Because it tends to obtain the images possessing visually similar pixel distributions, and the dataset contains numerous instances of clothes-changing, resulting in subpar performance. Text-only retrieval also falls short of expectations since most annotations in the dataset describe attire briefly, and there are numerous images with similar clothing. The combined use of both modalities in retrieval often yields the desired target images among the top results. When using the Word4Per method, the TINet, supervised with either \mathcal{L}_{Text} or \mathcal{L}_{Vis} , consistently succeeds in finding the target image. Case 2 exhibits a similar pattern to Case 1. However, in scenarios where the training dataset is unfiltered and remains consistent, as the textual information is more stable than visual one, thus TINet optimized with \mathcal{L}_{Text} tend to achieve the best retrieval results. On the contrary, the ambiguity of vision negatively effects the effectiveness of the model.

To demonstrate the effectiveness of the pseudo-word tokens generated by the TINet in capturing image information, another comparative experiment is conducted, as shown in Figure E. In this experiment, the pseudo-word tokens from all reference images are used to perform retrievals on a mixed dataset containing all reference images and gallery images. When employing the TINet supervised with \mathcal{L}_{Vis} , the model consistently finds the original image from the most similar retrieval results, even in situations where appearance of a person is highly consistent, as it leverages differences in the background. However, supervising with \mathcal{L}_{Text} , the original image cannot be located among the most similar retrieval results. This is mainly because semantic annotations for person images often do not focus on the background, but instead emphasize characteristics related to the individuals. It is also a key reason for

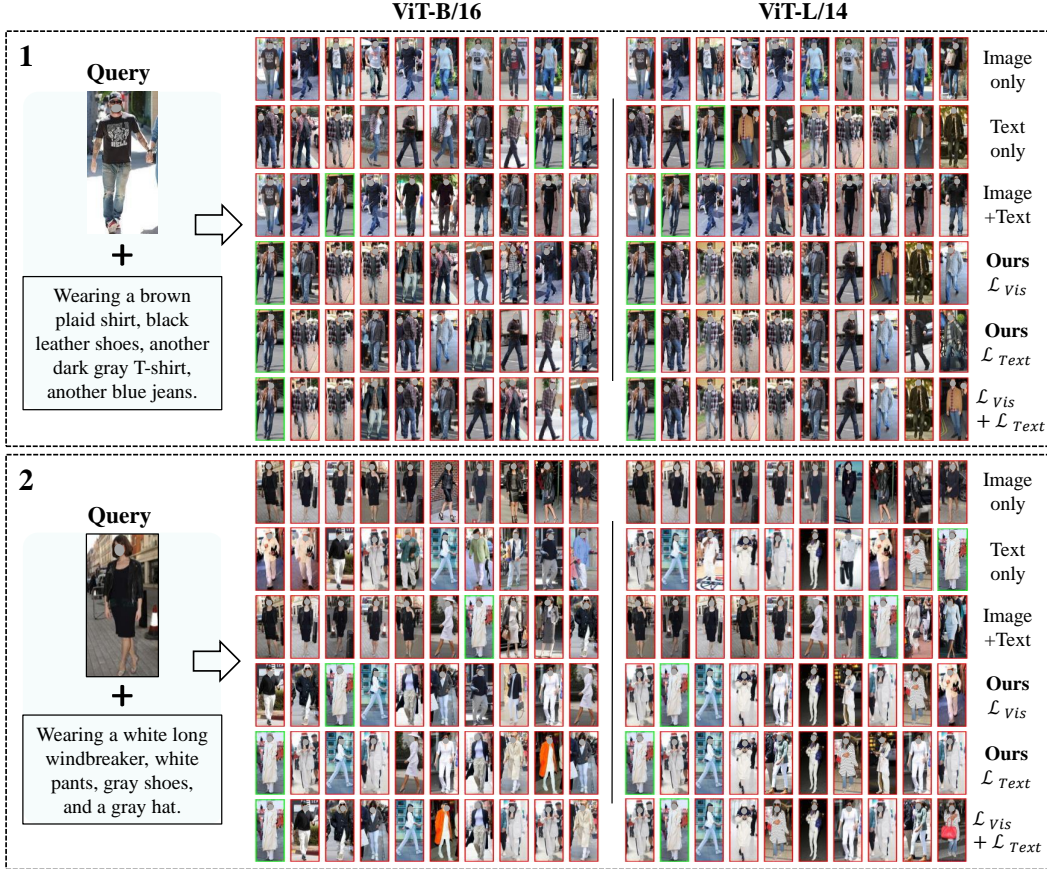


Figure D. Top-10 retrieval results on the ITCPR dataset for relevant methods. The figure presents retrieval results for two query examples under different methods, all employing encoders fine-tuned.

obtaining promising performance for the ZS-CPR task.

C.3. Ablation study for TINET architecture

In experiments, we use a consistent TINET setup (a three-layer fully connected network with a hidden layer width of 512). However, this setup may not be the most optimal configuration. Figure F illustrates the performance of TINets with different depths and hidden layer widths under various supervisions. We can see that a two-layer fully connected neural network is optimal for \mathcal{L}_{Vis} supervision, which differs from the previous setup. As for the hidden layer width, it is only sensitive to \mathcal{L}_{Text} supervision, and the optimal choice is 512. Considering a balance between efficiency and precision, we to keep the hidden layer width unchanged at 512.

C.4. Joint Training or Fusion.

Depending on the flexibility of Word4Per, during testing, the simultaneous utilization of multiple TINets for fusion retrieval is possible. The performance of the related methods on the ITCPR dataset is shown in Table B, in which TINET adopts the optimal structure (C.3). The comparisons

No.	Backbone	Method	Rank-1	Rank-5	Rank-10	mAP
1	ViT-B/16	\mathcal{L}_{Vis}	38.919	59.310	67.075	48.538
2		\mathcal{L}_{Text}	40.054	61.262	68.574	49.903
3		$\mathcal{L}_{Text} + \mathcal{L}_{Vis}$	39.464	61.308	68.483	49.728
4		No.1&2	40.872	61.989	68.847	50.521
5	ViT-L/14	\mathcal{L}_{Vis}	43.960	64.714	72.480	53.554
6		\mathcal{L}_{Text}	45.549	66.803	74.796	55.260
7		$\mathcal{L}_{Text} + \mathcal{L}_{Vis}$	45.095	64.759	72.480	54.162
8		No.5&6	45.913	66.848	75.114	55.630

Table B. Performance under different strategies. The symbol & in the method denotes fusion testing using the TINets of corresponding experiments.

between experiments No. 3 and No. 4, and experiments No. 7 and No. 8 illustrate that a fusion strategy generally tends to deliver superior performance compared to joint training. Notably, the performance of joint training even falls short of surpassing the performance of using a TINET optimized solely with \mathcal{L}_{Text} . In contrast, employing an appropriate fusion strategy often leads to the best performance and has

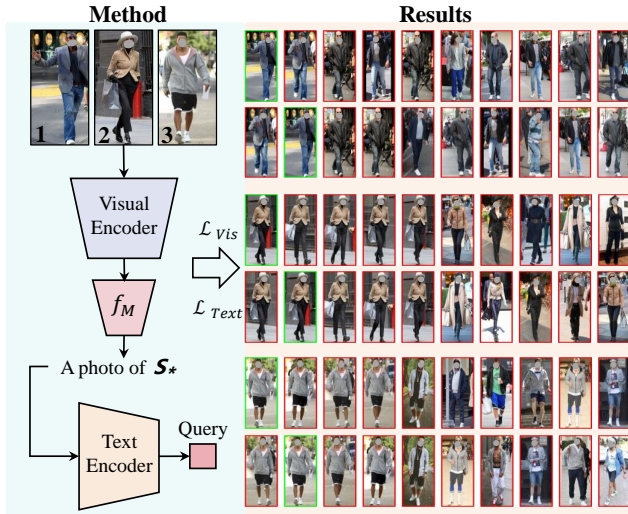


Figure E. Method and results of pseudo-word token retrieval for the original Image. On the left is an illustration of the retrieval method, and on the right are the retrieval results for three examples.

a broader range of choices.

C.5. Balancing Efficiency and Precision

In this section, we delve into how to achieve optimal performance based on the current framework, as well as the corresponding retrieval efficiency for different approaches. The relevant results are presented in Table C. By using the optimal text inversion network under the supervision of \mathcal{L}_{Vis} and training the extended data, experimental results No. 2-3 and No. 9-10 are obtained. This represents the optimal performance achievable with a single textual inversion network. A substantial improvement is achieved when employing two textual inversion networks for fusion (No. 4-6 and No. 11-13). Among them, the TINets using the same supervision optimization have the smallest fusion improvement (No. 6 and No. 13), even if their single network performance is outstanding. Further gains in performance are achieved when using three textual inversion networks, albeit to a lesser extent (No. 7 and No. 14). It can thus be inferred that fusing more well-trained textual inversion networks leads to better performance, though the degree of improvement diminishes. Moreover, examining the variations in inference time in the table indicates that using more textual inversion networks is accompanied by a reduction in retrieval efficiency. When applying this method, it is crucial to flexibly select a fusion scheme based on the specific practical application scenario.

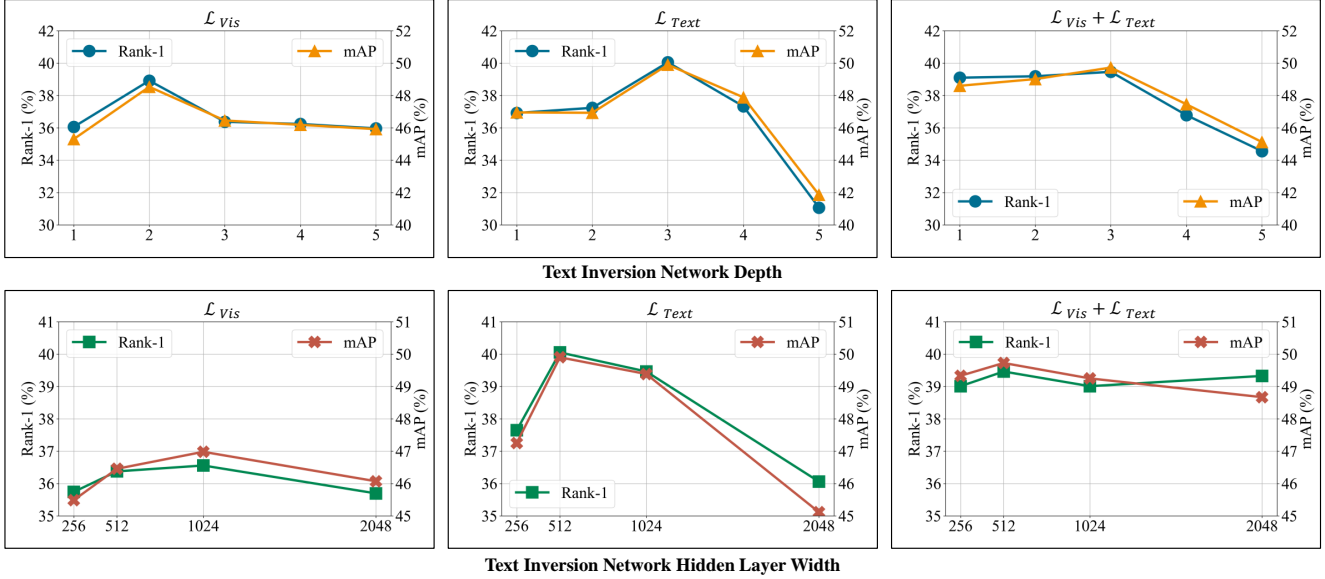


Figure F. Method performance using TINet with different depths and hidden layer widths under various supervisions. **Top**: Performance using TINet with different depths, with a hidden layer width of 512. **Bottom**: Performance using TINet with different hidden layer widths, all with a depth of three layers.

No.	Backbone	Dataset	Method	Time (s)	Rank-1	Rank-5	Rank-10	mAP
1	ViT-B/16	C	\mathcal{L}_{Text}	30.656	40.054	61.262	68.574	49.903
2		$C + I + R$	\mathcal{L}_{Vis}	30.454	41.826	62.307	69.391	51.353
3		$IPR^{10\%+}$	\mathcal{L}_{Vis}	30.453	41.508	62.080	69.028	50.825
4		-	$No.1\&2$	31.020	43.415	63.442	70.663	52.740
5		-	$No.1\&3$	31.081	43.415	63.488	70.754	52.622
6		-	$No.2\&3$	30.997	42.461	63.124	70.481	52.073
7		-	$No.1\&2\&3$	31.574	43.551	63.760	71.026	53.041
8	ViT-L/14	C	\mathcal{L}_{Text}	65.130	45.549	66.803	74.796	55.260
9		$C + I + R$	\mathcal{L}_{Vis}	64.986	45.595	65.168	72.616	54.755
10		$IPR^{10\%+}$	\mathcal{L}_{Vis}	64.979	45.549	66.167	73.025	54.906
11		-	$No.1\&2$	66.063	47.184	68.256	75.023	56.790
12		-	$No.1\&3$	66.069	47.048	68.483	74.796	56.636
13		-	$No.2\&3$	65.913	46.458	66.803	74.069	55.688
14		-	$No.1\&2\&3$	66.475	47.502	68.392	75.103	56.944

Table C. Performance under different strategies. The time in the table represents the duration required for the respective method to complete all retrieval tasks on the entire ITCPR dataset, thus avoiding potential statistical anomalies.